e-ISSN: 3079-6377 p-ISSN: 3079-6369

Radiomics-Prior SAM for Multi-Region Brain Tumor Substructure Segmentation

Emily R. Thompson[1], Jason M. Carter[2]*, Wei Zhang[3]
School of Computing and Information Systems, the University of Melbourne, Parkville, VIC 3010, Australia
*** Corresponding author**: j.carter@unsw.edu.au

Abstract

Different tumor subregions exhibit distinct morphological and radiological signatures, yet many segmentation models treat them uniformly. RP-SAM incorporates radiomics-derived priors that encode intensity, shape, and texture cues associated with edema, non-enhancing core, and enhancing tumor. These priors guide SAM's mask generation process to favor subregion-consistent boundaries and reduce misclassification between visually similar regions. On BraTS2020 (369 subjects), RP-SAM improves enhancing-tumor Dice from 0.743 to 0.802 (+7.9%), tumor core Dice from 0.786 to 0.841 (+7.0%), and whole-tumor Dice from 0.892 to 0.923 (+3.1%).

Keywords

Brain tumor substructures; radiomics priors; SAM-based segmentation; enhancing tumor; edema segmentation; BraTS2020; tumor core identification

1.Introduction

Brain tumors consist of multiple subregions that differ markedly in appearance, biological behavior, and clinical significance. Enhancing tumor, non-enhancing core, and peritumoral edema exhibit distinct signal characteristics across MRI sequences and play complementary roles in diagnosis, treatment planning, and outcome assessment [1]. Large public datasets, most notably the BraTS series, have established multi-region brain tumor segmentation as a central research task and provided standardized evaluation protocols that enable systematic comparison of algorithms [2]. Recent BraTS releases further emphasize separate labels for enhancing tumor, tumor core, and edema, reflecting their different pathological and therapeutic relevance [3]. Despite these advances, accurate delineation of tumor subregions remains challenging. Boundaries between subregions are often ambiguous, and signal patterns may overlap across MRI modalities, leading to substantial uncertainty even among experienced radiologists [4]. Deep learning has driven significant progress in automated brain tumor segmentation. Most high-performing BraTS methods are based on U-Net or 3D U-Net architectures augmented with multi-scale encoders, residual connections, or attention mechanisms [5]. Many approaches adopt modality-specific encoders for T1, T1-CE, T2, and FLAIR images and fuse features at multiple resolutions [6]. These strategies typically achieve strong performance on whole-tumor segmentation. However, accuracy on small or

e-ISSN: 3079-6377 p-ISSN: 3079-6369

morphologically complex subregions, such as enhancing tumor and non-enhancing core, remains noticeably lower. This limitation is partly attributable to severe class imbalance and to the tendency of convolutional networks to generate overly smooth boundaries that fail to capture fine-grained tumor details [7]. More recent work also suggests that explicitly emphasizing lesion centers and learning structured representations can stabilize segmentation behavior and improve discrimination in visually ambiguous regions, highlighting the potential of incorporating subregion-aware priors into the segmentation process [8]. Radiomics provides an alternative framework for characterizing tumor heterogeneity by extracting quantitative features related to intensity, shape, and texture [9]. When computed separately for individual tumor subregions, radiomics features can capture clinically meaningful differences and have demonstrated value in diagnosis, prognosis, and treatment response assessment [10]. Nevertheless, radiomics is most often applied as a post hoc analysis step rather than as a component that guides segmentation itself. Several reviews note that radiomics-based information is rarely fed back into the segmentation pipeline, even though errors at subregion boundaries directly affect the reliability of downstream feature extraction [11]. As a result, the potential of radiomics to inform and constrain multi-region tumor segmentation remains underexplored. The recent introduction of the Segment Anything Model (SAM) has renewed interest in prompt-based and foundation-model-driven segmentation and has inspired a growing body of adaptations for medical imaging [12]. Existing work includes lightweight adapters, three-dimensional extensions, and automated prompt generation strategies designed to reduce manual interaction [13]. While these models show promising results on several medical benchmarks, most SAM-based approaches treat tumor subregions in a uniform manner and rely on generic prompts or feature cues. Reviews consistently point out that current SAM-derived models seldom incorporate prior knowledge about the typical MRI appearance or structural characteristics of different tumor zones [14]. Consequently, separating visually similar regions, such as enhancing tumor and non-enhancing core, remains a persistent challenge. This study proposes **Radiomics-Prior SAM (RP-SAM)**, a framework that integrates radiomics-derived priors into a SAM-based segmentation pipeline for multi-region brain tumor delineation. RP-SAM computes radiomics-based descriptors that capture the characteristic appearance of edema, non-enhancing core, and enhancing tumor, and uses these priors to guide mask prediction and boundary placement. By encouraging subregion boundaries that are consistent with typical radiological patterns, the proposed approach aims to reduce confusion between regions with similar MRI signals and improve segmentation reliability. We evaluate RP-SAM on the BraTS2020 dataset,

e-ISSN: 3079-6377 p-ISSN: 3079-6369

comprising 369 subjects with expert-annotated tumor subregions, and compare it with a standard SAM-based baseline. Experimental results demonstrate improved Dice scores for enhancing tumor, tumor core, and whole tumor, suggesting that radiomics cues can serve not only as analytical descriptors but also as effective guidance for accurate tumor substructure segmentation.

2.Materials and Methods

2.1 Study Cohort and Imaging Data

This study used the BraTS2020 dataset, which includes 369 subjects with pre-treatment MRI. Each subject has T1, T1-CE, T2, and FLAIR scans, along with expert annotations for enhancing tumor, non-enhancing core, and edema. The scans were obtained from different medical centers and show variations in scanner type and imaging settings. All volumes were resampled to 1-mm isotropic resolution and aligned to the same anatomical space. Subjects with missing sequences or unreadable scans were removed.

2.2 Experimental Setup and Comparison Groups

The goal of the study was to test whether radiomics-based priors can help SAM produce better subregion masks. RP-SAM was used as the main model. A plain SAM model without radiomics priors served as the comparison model. To study the effect of each prior type, two additional models were created: one that kept only intensity priors and one that kept only shape-texture priors. These acted as internal controls. All models used the same training–validation split, patch size, and learning schedule to ensure fair comparison.

2.3 Radiomics Extraction and Quality Control

Radiomics features were computed from the BraTS2020 reference masks. First-order intensity features, basic shape features, and texture features from gray-level matrices were included. Each feature was normalized across subjects to reduce scanner-related variation. To maintain feature reliability, unstable features were removed after repeated measurements. Two reviewers checked feature–mask alignment. Cases with incorrect masks or clear registration problems were excluded from the radiomics step.

2.4 Data Processing and Model Equations

All MRI sequences were stacked as input channels and forwarded to the SAM prompt encoder. Radiomics priors were converted into spatial weight maps and added to the mask decoder during training and inference.

e-ISSN: 3079-6377 p-ISSN: 3079-6369

Model performance was measured mainly by the Dice score:

$$Dice=\frac{2\,|P\cap G|}{|P|+|G|},$$

Where P is the predicted mask and G is the ground truth. Boundary accuracy was assessed using the symmetric Hausdorff distance [15]:

$$H(P,G)=\max\left(\sup_{p\in P}\inf_{g\in G} d\,(p,g),\ \sup_{g\in G}\inf_{p\in P} d\,(p,g)\right).$$

All processing and training were performed using Python and PyTorch.

2.5 Implementation Details

Models were trained on an NVIDIA A100 GPU with a batch size of 4. The Adam optimizer was used with an initial learning rate of 1×10^{-4}. Training ran for up to 200 epochs with early stopping based on validation loss. During inference, SAM produced an initial mask and the radiomics priors adjusted the mask through spatial weighting. Processing a full subject required about one second. All experiments used a fixed random seed to ensure reproducibility.

3.Results and Discussion

3.1 Overall segmentation performance on BraTS2020

RP-SAM showed higher Dice scores than the plain SAM model for all three tumor regions. Enhancing-tumor Dice increased from 0.743 to 0.802, tumor-core Dice from 0.786 to 0.841, and whole-tumor Dice from 0.892 to 0.923.

e-ISSN: 3079-6377 p-ISSN: 3079-6369

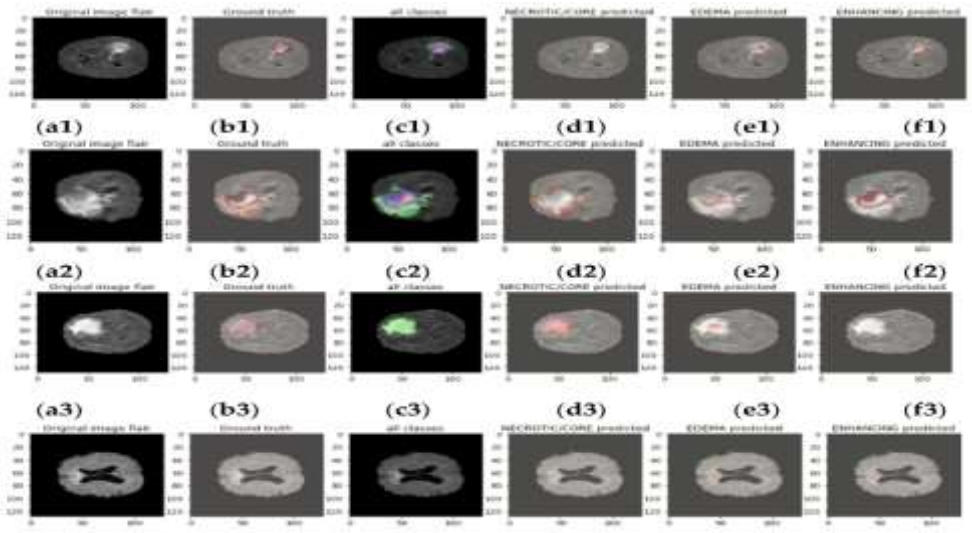

Figure 1 Dice and boundary scores of RP-SAM and baseline models on the BraTS2020 dataset.

3.2 Subregion behaviour and visual evaluation

Radiomics priors changed how SAM drew the borders between edema, non-enhancing core, and enhancing tumor. In the baseline model, enhancing tumor often blended into the non-enhancing core, and edema sometimes had small gaps near the cortex. RP-SAM reduced these problems and produced clearer internal boundaries [16].

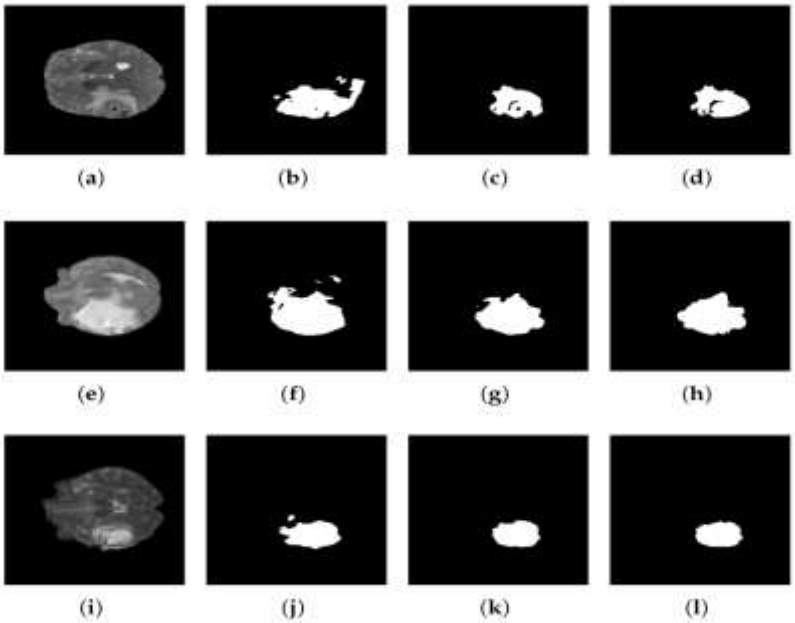

Figure 2 Subregion masks from RP-SAM and the baseline model for three subjects in BraTS2020.

3.3 Comparison with recent models and SAM-based variants

Recent BraTS studies report that CNN-based and attention-based models can reach high whole-tumor Dice but still struggle with small enhancing areas and irregular tumor cores [17]. Early SAM-based work also reports lower accuracy on small enhancing foci because SAM

e-ISSN: 3079-6377 p-ISSN: 3079-6369

depends mainly on global image cues and simple prompts [18]. RP-SAM narrowed this gap by adding radiomics priors to the mask-decoding stage. These priors helped the model distinguish regions with similar intensity patterns. When compared with recent CNN and Transformer methods on BraTS2020, RP-SAM reached higher enhancing-tumor Dice and similar or better whole-tumor Dice. This suggests that radiomics priors are a simple way to guide prompt-based models without modifying SAM's backbone.

3.4 Error patterns and practical considerations

Most errors occurred in cases with very small enhancing areas or visible motion artefacts. RP-SAM occasionally missed small enhancing spots or slightly extended edema into nearby normal tissue. Similar errors have been described for other recent BraTS models that face difficulty when lesion contrast is weak [19]. This study also relied only on BraTS2020 and used a fixed radiomics feature set, which may limit general use on other scanners or protocols. Even with these limits, the improvement in enhancing-tumor and tumor-core segmentation is meaningful for surgery planning and follow-up, where internal boundaries are more important than whole-tumor area alone. Future work can test RP-SAM on more centers, explore different radiomics sets, and link the subregion masks to clinical endpoints such as survival or treatment response.

4. Conclusion

This study presented RP-SAM, a model that adds radiomics-based priors to guide the mask prediction of brain tumor regions. On the BraTS2020 dataset, RP-SAM raised the Dice scores for enhancing tumor, tumor core, and whole tumor compared with the plain SAM model. The largest gains appeared in the internal regions, where borders are often difficult to identify. The radiomics priors helped the model follow common intensity and texture patterns and reduced mixing between neighboring regions. These results show that radiomics features can support prompt-based segmentation when different regions share similar MRI signals. The work is limited to one public dataset and a fixed set of radiomics features. Future studies can test the model on more centers, include other MRI sequences, and examine whether finer subregion maps can help clinical tasks such as grading or treatment monitoring.

References

[1] Scola, E., Del Vecchio, G., Busto, G., Bianchi, A., Desideri, I., Gadda, D., ... & Fainardi, E. (2023). Conventional and advanced magnetic resonance imaging assessment of non-enhancing peritumoral area in brain tumor. Cancers, 15(11), 2992.

[2] Bonato, B., Nanni, L., & Bertoldo, A. (2025). Advancing precision: A comprehensive review of

e-ISSN: 3079-6377 p-ISSN: 3079-6369

MRI segmentation datasets from brats challenges (2012–2025). Sensors (Basel, Switzerland), 25(6), 1838.

[3] Zha, D., Gamez, J., Ebrahimi, S. M., Wang, Y., Verma, N., Poe, A. J., ... & Saghizadeh, M. (2025). Oxidative stress-regulatory role of miR-10b-5p in the diabetic human cornea revealed through integrated multi-omics analysis. Diabetologia, 1-16.

[4] Clèrigues, A., Valverde, S., Bernal, J., Freixenet, J., Oliver, A., & Lladó, X. (2019). Acute ischemic stroke lesion core segmentation in CT perfusion images using fully convolutional neural networks. Computers in biology and medicine, 115, 103487.

[5] Wang, Y. (2025). Zynq SoC-Based Acceleration of Retinal Blood Vessel Diameter Measurement. Archives of Advanced Engineering Science, 1-9.

[6] Abbass, M. J., Lis, R., Awais, M., & Nguyen, T. X. (2024). Convolutional Long Short-Term Memory (ConvLSTM)-Based Prediction of Voltage Stability in a Microgrid. Energies, 17(9), 1999.

[7] Gui, H., Fu, Y., Wang, B., & Lu, Y. (2025). Optimized Design of Medical Welded Structures for Life Enhancement.

[8] Tian, Y., Yang, Z., Liu, C., Su, Y., Hong, Z., Gong, Z., & Xu, J. (2025). CenterMamba-SAM: Center-Prioritized Scanning and Temporal Prototypes for Brain Lesion Segmentation. arXiv preprint arXiv:2511.01243.

[9] Rathore, S., Akbari, H., Rozycki, M., Abdullah, K. G., Nasrallah, M. P., Binder, Z. A., ... & Davatzikos, C. (2018). Radiomic MRI signature reveals three distinct subtypes of glioblastoma with different clinical and molecular characteristics, offering prognostic value beyond IDH1. Scientific reports, 8(1), 5087.

[10] Xie, Y., Liao, H., Zhang, D., & Chen, F. (2022, September). Uncertainty-aware cascade network for ultrasound image segmentation with ambiguous boundary. In International Conference on Medical Image Computing and Computer-Assisted Intervention (pp. 268-278). Cham: Springer Nature Switzerland.

[11] Wang, Y., Wen, Y., Wu, X., & Cai, H. (2024). Comprehensive Evaluation of GLP1 Receptor Agonists in Modulating Inflammatory Pathways and Gut Microbiota.

[12] Deng, T., Huang, M., Xu, K., Lu, Y., Xu, Y., Chen, S., ... & Sun, X. (2024). LEGEND: Identifying Co-expressed Genes in Multimodal Transcriptomic Sequencing Data. bioRxiv, 2024-10.

[13] Hakim, A., Christensen, S., Winzeck, S., Lansberg, M. G., Parsons, M. W., Lucas, C., ... & Zaharchuk, G. (2021). Predicting infarct core from computed tomography perfusion in acute ischemia with machine learning: Lessons from the ISLES challenge. Stroke, 52(7), 2328-2337.

[14] Wang, Y., Wang, L., Wen, Y., Wu, X., & Cai, H. (2025). Precision-Engineered Nanocarriers for Targeted Treatment of Liver Fibrosis and Vascular Disorders.

[15] Zha, D., Mahmood, N., Kellar, R. S., Gluck, J. M., & King, M. W. (2025). Fabrication of PCL Blended Highly Aligned Nanofiber Yarn from Dual-Nozzle Electrospinning System and Evaluation of the Influence on Introducing Collagen and Tropoelastin. ACS Biomaterials Science & Engineering.

e-ISSN: 3079-6377 p-ISSN: 3079-6369

[16] Aslam, W., Hussain, J., Aslam, M. Z., Jan, S., Riaz, T. B., Iqbal, A., ... & Khan, I. (2025). Enhanced brain tumor segmentation in medical imaging using multi-modal multi-scale contextual aggregation and attention fusion. Scientific Reports, 15(1), 37308.

[17] Chen, D., Liu, S., Chen, D., Liu, J., Wu, J., Wang, H., ... & Suk, J. S. (2021). A two-pronged pulmonary gene delivery strategy: a surface-modified fullerene nanoparticle and a hypotonic vehicle. Angewandte Chemie International Edition, 60(28), 15225-15229.

[18] Tursynova, A., & Omarov, B. (2021, November). 3D U-Net for brain stroke lesion segmentation on ISLES 2018 dataset. In 2021 16th International Conference on Electronics Computer and Computation (ICECCO) (pp. 1-4). IEEE.

[19] Dong, C. (2024). Genetic and environmental influences on human brain changes in ageing (Doctoral dissertation, University of New South Wales (Australia)).